VOL. 5, NO. 10, OCTOBER 2010 ISSN 1819-6608
ARPN Journal of Engineering and Applied Sciences


www.arpnjournals.com

THERMODYNAMIC PROPERTIES OF BINARY MIXTURE FOR POWER GENERATION SYSTEMS

N. Shankar Ganesh and T. Srinivas
Vellore Institute of Technology, Vellore, India
E-Mail: nshankar_g@rediffmail.com

ABSTRACT

In Kalina power generation as well as vapor absorption and refrigeration systems ammonia-water mixture has been used as working fluids. Unlike for pure components, binary mixtures additionally need mixture concentration to solve thermodynamic properties. A flowchart is developed to understand the computations of the properties. The thermodynamic properties for ammonia-water mixture have been generated using MATLAB computer code. The solved properties are bubble point temperature, dew point temperature, specific enthalpy, specific entropy, specific volume and exergy. The property charts i.e. enthalpy-concentration, entropy-concentration, temperature-concentration and exergy-concentration charts have been prepared. The present work can be used to simulate the power generating systems to get the feasibility of the proposed ideas up to 100 bar. This work can be used to carry out the exergy analysis of Kalina power cycles.

Keywords: thermodynamic, ammonia-water mixture, power generation.

INTRODUCTION

Enthalpy, entropy, internal energy, exergy, fugacity etc. are useful thermodynamic properties to analyze the energy and exergy systems. These properties can be used to study the parametric variations in the systems. It is therefore important to extend such property variations as the temperature, pressure and other independent variables of a system change.

In studying vapor-liquid equilibrium for binary mixtures, there are four intensive variables which will concern are temperature, pressure, single liquid mole fraction and single vapor mole fraction [1]. To find out the performance of power cycles these thermodynamic properties play a vital role. For determining the thermodynamic properties of ammonia-water mixture various mathematical correlations are used.

In ammonia-water mixture ammonia has got low boiling point which makes it useful for utilizing the waste heat source and makes possibility of boiling at low temperature. Ammonia-water mixture as non-azeotropic nature will have the tendency to boil and condense at a range of temperatures which possess a closer match between heat source and working fluid mixture. The similar molecular weight of ammonia as that of water, make it possible to utilize the standard steam turbine components.

In 1984 Ziegler and Trepp [2] described an equation for the thermodynamic properties of ammonia-water mixture in absorption units. In his work the Gibbs excess energy equation was utilized for determining the specific enthalpy, specific entropy and specific volume. They developed the properties up to a pressure of 50 bar and temperature of 500 K. Renon [3] derived an equation of state which shows a good representation of the ammonia-water system. Redlick-Kwong equation of state was utilized and with two adjusted parameters gives a representation of vapor liquid equilibrium (VLE) for the ammonia-water system. In his work it was reported to a pressure up to 7 MPa. The two adjusted parameters were: First, acentric factor and a polar parameter characteristic of substance were adjusted for each pure component on pure vapor pressure data and second, the four K_{ij} parameters were adjusted on vapor liquid equilibrium. Simplified thermodynamic description of mixtures and solutions by Ruiter [4] presented a simplified thermodynamic model for mixtures and solutions. The equilibrium pressure and the excess enthalpy of mixtures and solutions were thermodynamically described by 11 coefficients. Patek and Klomfar [5] developed five equations describing VLE properties of ammonia-water system which were intended for use in the design of absorption processes. With these equations iterative evaluations have been avoided. The equations presented can be used to calculate initial values for a constant formulation. According to Hasan Orbey [6], combination of activity coefficient models with equations of state both at infinite pressure and at zero pressure were presented. These mixing rules were successful for some range of temperatures. For ammonia-water mixture many researchers have worked on Gibbs excess energy equation. According to Abovsky [7] perturbation theory will fit the entire set of experimental data for thermodynamic properties of pure components and their mixture. He utilized the perturbation theory in a wide range of temperature [200 - 640 K] and pressure [0.02 - 23 MPa].

Najjar [8] has selected two constant - equation of state, such as the Soave-Redlick-Kwong and Peng-Robison equations as the simplest among many equations of state. With the two equations thermodynamic properties such as pressure, internal energy, enthalpy, entropy for ammonia in the superheated region was predicted. In application of the extended corresponding states method an application of the one-fluid extended corresponding states method to the calculation of the thermodynamic surface of the ammonia-water mixture were presented [9]. For pure ammonia and water Haar-Gallaghar and Prub-Wagner equations of state were chosen. The estimation of the binary interaction parameters was performed using the

general case of the least square method. Tillner Roth and Friend [10] in their presentation a fundamental equation of state for the Helmholtz free energy of the mixture (water-ammonia) which covers the thermodynamic space between the solid-liquid-vapor boundary and the critical locus which is valid in the vapor and liquid phases for pressures up to 40 MPa with an uncertainty of ± 0.01 in liquid and vapor mole fractions. Goswami [11] discussed a method which uses Gibbs excess free energy equations for pure ammonia and water properties, and empirical bubble and dew point temperature equations for VLE. This method avoids the iterations necessary for calculating bubble point temperature (BPT) and dew point temperature (DPT) by the fugacity method.

In potential applications of artificial neural networks to thermodynamics the potential application of neurocomputing for estimating vapor-liquid equilibrium data has been explored [12]. The associative property of artificial neural networks for the prediction of vapor-liquid equilibrium has been explores using back propagation algorithm. Weber [13] in his work estimated the second and third virial coefficients B and C for the mixture utilizing corresponding states model applied successfully to pure fluids, binary and ternary mixtures. Lemmon and Roth [14] developed a new approach for calculating the properties of mixtures based on an equation of state in reduced Helmholtz energy which allows for the representation of the thermodynamic properties over a wide range of fluid states and is based on highly accurate equations of state for the pure components combined at the reduced temperature and density of the mixture. In modeling of the thermodynamic properties of the ammonia-water mixture a three constant Margules model of the excess free enthalpy was formulated for the liquid phase [15]. The vapor phase was considered as a perfect mixture of real gases, and each pure gas being described by a virial equation of state. The model developed shows good accuracy for temperature from 200 to 800 K and pressures up to 100 bar. Mejbri and Bellage [16] have presented three different approaches. The first is an empirical approach based on a free enthalpy model of the mixture. Secondly a semi-empirical approach based on Patel and Teja cubic equation of state was considered. Finally, a theoretical approach formulated as PC-SAFT (Perturbed chain statistical associating fluid theory) equation of state was treated. Soleimani [17] in his work presented a set of five simple equations and explicit functions for the determination of the vapor-liquid equilibrium properties of the ammonia-water mixture. The functions were constructed by the least square method for curve fitting. The presented functions are valid up to 140^{o}C and 100 bar.

The main objectives of the present work are to develop the property up to exergy level without iterations and with simple and easy calculations. The presented work can be used for energy and exergy solutions to power generating systems. The exergy details and its concentration graph for the ammonia water mixtures are not reported out in the literature which is the gap identified and presented at various pressures. The results were simulated using MATLAB which avoids numerous procedures for programming.

THERMODYNAMIC EVALUATION OF NH_3-H_2O MIXTURE PROPERTIES

For ammonia-water mixture to calculate the thermodynamic properties like specific enthalpy, specific entropy and specific volume the need of bubble and dew point temperatures at various pressures and compositions are very essential and is the prior step. For estimating those temperatures various correlations have been developed. The correlation developed by Patek and Klomfar [5] is proposed in this work which avoids tedious iterations required by the complicated method fugacity coefficient of a component in a mixture and the correlation proposed by Ibrahim and Klein [19].

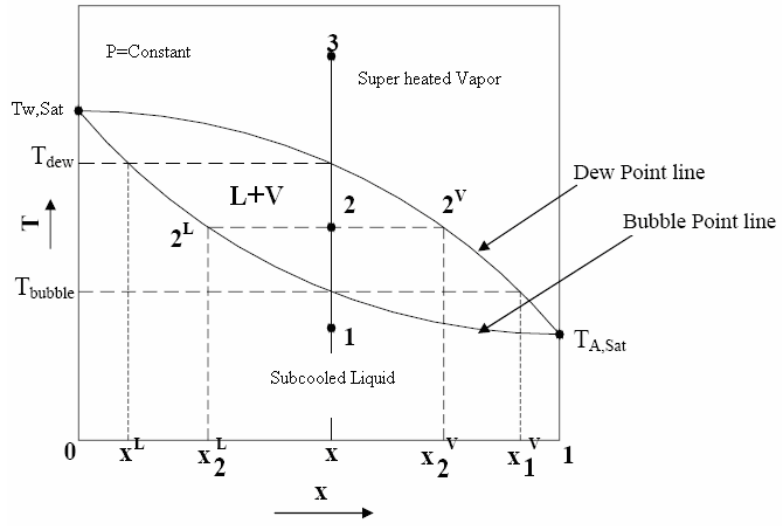

Figure-1. Temperature-concentration curve for NH3- H2O at constant pressure.

Figure-1. shows the details of bubble point and dew point temperature variations with ammonia concentration. The loci of all the bubble points are called as the bubble point line and the loci of all the dew points are called as the dew point line. The bubble point line is the saturated liquid line and the region between the bubble and dew point lines is the two phase region where both liquid and vapor coexist in equilibrium [20].

A. Calculating Bubble and Dew point temperatures

$$T_b(p,x) = T_o \sum_i a_i (1-x)^{m_i} \left[\ln\left(\frac{p_o}{p}\right) \right]^{n_i} \quad (1)$$

$$T_d(p,y) = T_o \sum_i a_i (1-y)^{m_i/4} \left[\ln\left(\frac{p_o}{p}\right) \right]^{n_i} \quad (2)$$

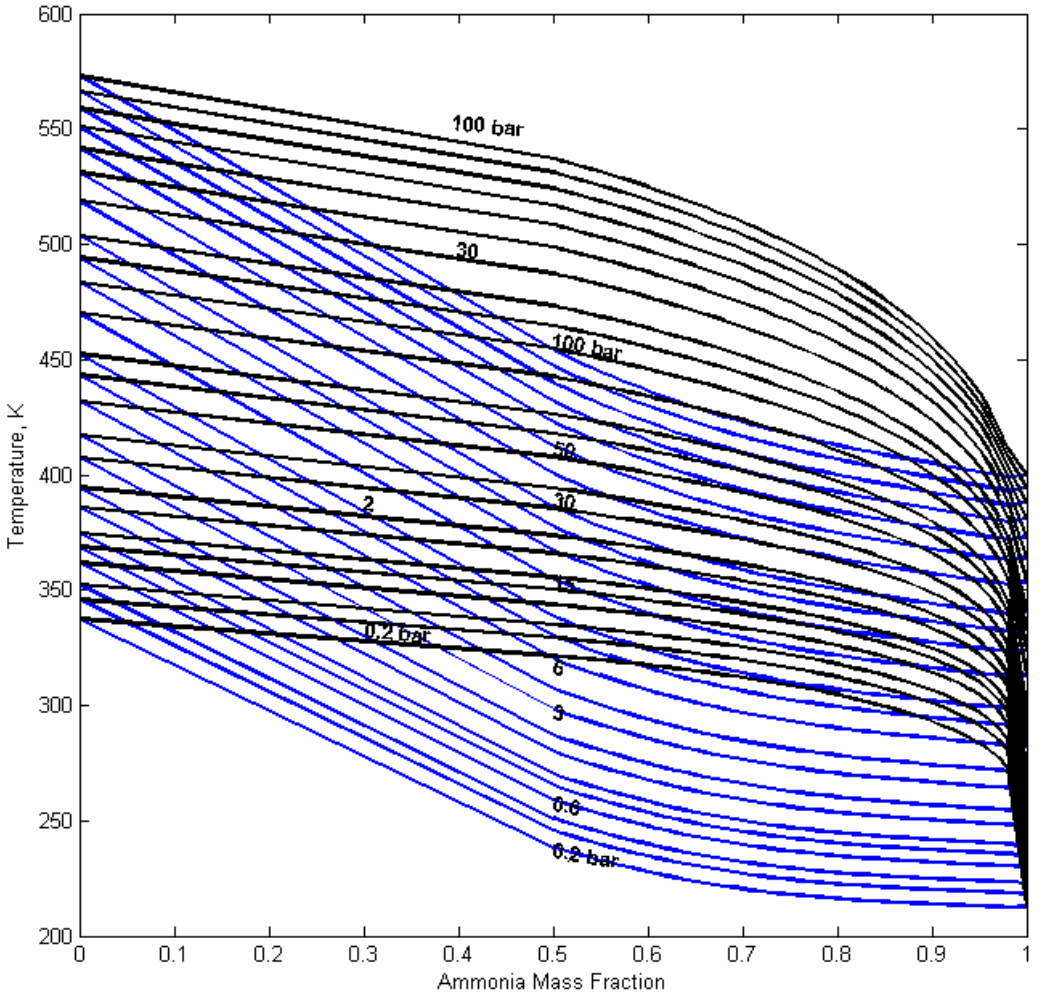

Figure-2. Bubble and dew point temperatures up to100 bar pressure.

Figure-2 shows the bubble and dew point temperatures developed with the correlation by Patek and Klomfar [5] up to pressure of 100 bar using MATLAB code. The obtained results were compared with the literature and produced the similar results up to 50 bars and deviated to a small percent from 50 bar to 100 bar pressure [4]. A flowchart is prepared to understand the mathematical calculations for properties.

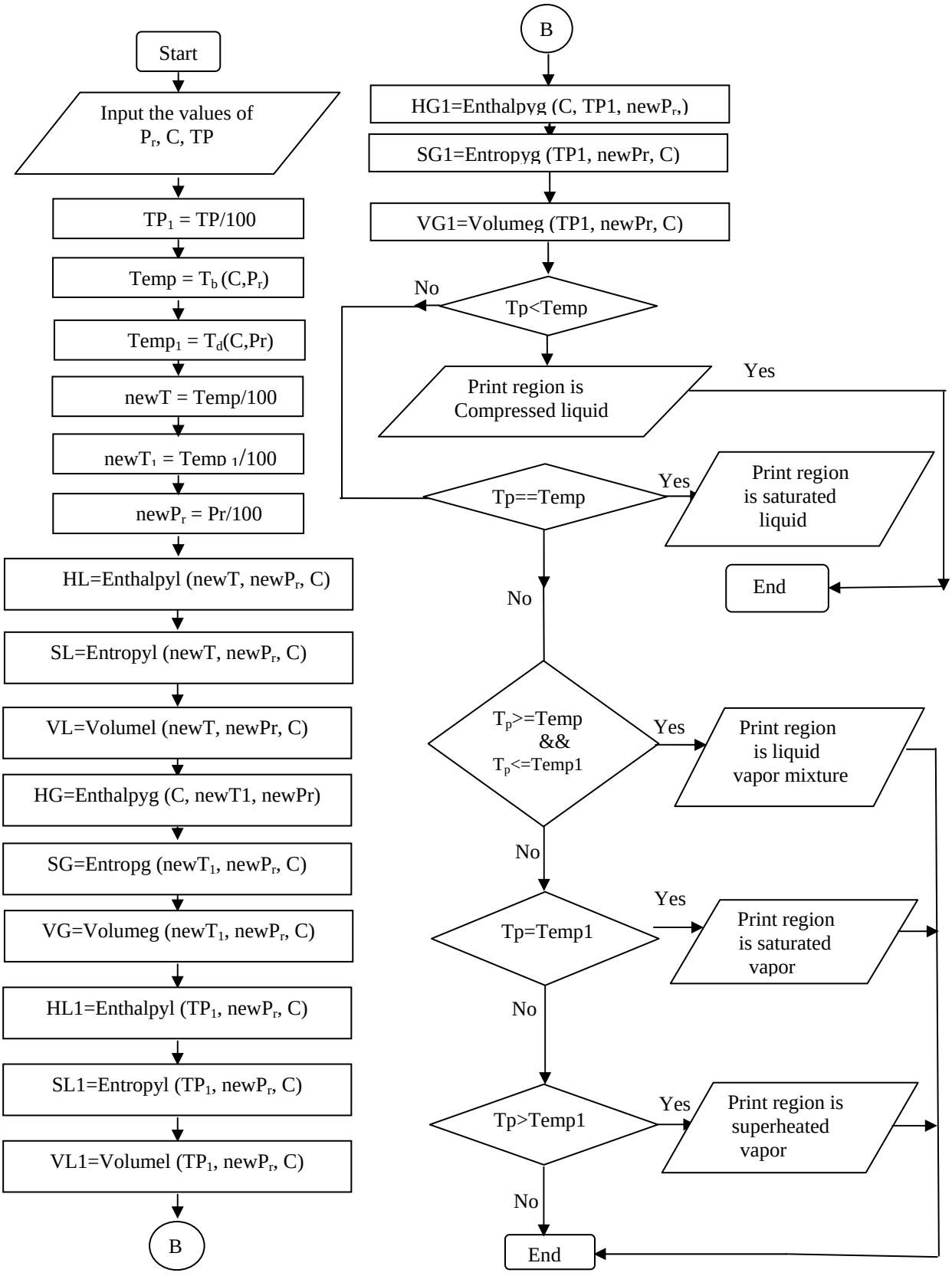

Figure-3. Flowchart to find thermodynamic properties of mixture.

Development of equations

The properties are derived from Gibbs free energy function. The coefficients used are given in Table-1 and Table-2.

Table-1. Coefficients for the equations for the pure components.

Coefficient	Ammonia	Water
a_1	3.971423 E-2	2.748796 E-2
a_2	-1.790557 E-5	-1.016665 E-5
a_3	-1.308905 E-2	- 4.452025 E-3
a_4	3.752836 E-3	8.389246 E-4
b_1	1.634519 E1	1.214557 E1
b_2	-6.508119	- 1.898065
b_3	1.448937	2.911966 E-1
c_1	-1.049377 E-2	2.136131 E-2
c_2	-8.288224	- 3.169291 E1
c_3	-6.647257 E2	-4.634611 E4
c_4	-3.045352 E3	0.0
d_1	3.673647	4.019170
d_2	9.989629 E-2	-5.175550 E-2
d_3	3.617622 E-2	1.951939 E-2
h^l	4.878573	21.821141
h^g	26.468879	60.965058
s^l	1.644773	5.733498
s^g	8.339026	13.453430
T_o	3.2252	5.0705
p_o	2.0000	3.0000

Table-2. Coefficients for the gibbs excess energy function.

e_1	-4.626129 E1
e_2	2.060225 E-2
e_3	7.292369
e_4	-1.032613 E-2
e_5	8.074824 E1
e_6	-8.461214 E1
e_7	2.452882 E1
e_8	9.598767 E-3
e_9	-1.475383
e_{10}	-5.038107 E-3
e_{11}	-9.640398 E1
e_{12}	1.226973 E2
e_{13}	-7.582637
e_{14}	6.012445 E-4
e_{15}	5.487018 E1
e_{16}	-7.667596 E1

For the liquid phase the Gibbs free energy equation is given below:

$$g^{l}_{(T,p,x)} = \left\{(1-x)g^{l}H_2O_{(T,p)} + x\,g^{l}NH_{3(T,p)} + RT\left[(1-x)\log_e(1-x) + x\log_e x\right] + g_{E(T,p,x)}\right\} \quad (3)$$

$$g^{l}_{H_2O_{(T,p)}} = \left[h^{l}(T_o,p_o) - Ts^{l}(T_o,p_o) + \int c^{l}_{p}dT - T\int \frac{c^{l}_{p}}{T}dT + \left(a_1 + a_3T + a_4T^2\right)(p-p_o) + a_2\frac{\left(p^2 - {p_o}^2\right)}{2}\right]_{H_2O} \quad (4)$$

Where

$$c^{l}_{p(T,po)} = b_1 + b_2T + b_3T^2$$

After simplification of the above equations (3 and 4)

$$g^{l}_{H_2O_{(T,p)}} = \left\{h^{l}(T_o,p_o) - Ts^{l}(T_o,p_o) + \left[b_1(T-T_o) + \frac{b_2}{2}\left(T^2 - {T_o}^2\right) + \frac{b_3}{3}\left(T^3 - {T_o}^3\right)\right] + \left[\left(a_1 + a_3T + a_4T^2\right)(p-p_o) + a_2\frac{\left(p^2 - {p_o}^2\right)}{2}\right]\right\}_{H_2O} \quad (5)$$

$$g^{l}_{NH_{3(T,p)}} = \left\{h^{l}_{(T_o,p_o)} - Ts^{g}(T_o,p_o) + \left[b_1(T-T_o) + \frac{b_2}{T}\left(T^2 - {T_o}^2\right) + \frac{b_3}{3}\left(T^3 - {T_o}^3\right)\right] + \left[\left(a_1 + a_3T + a_4T^2\right)(p-p_o) + a_2\frac{\left(p^2 - {p_o}^2\right)}{2}\right]\right\}_{NH_3} \quad (6)$$

$$g_{E(T,p,x)} = \left\{\begin{array}{l}\left(e_1 + e_2p + (e_3 + e_4p)T + \frac{e_5}{T} + \frac{e_6}{T^2}\right) + (2x-1)\left(e_7 + e_8p + (e_9 + e_{10}p)T + \frac{e_{11}}{T} + 3\frac{e_{12}}{T^2}\right) + \\ (2x-1)^2\left(e_{13} + e_{14}p + \frac{e_{15}}{T} + \frac{e_{16}}{T^2}\right)\end{array}\right\} \quad (7)$$

For the gas phase the Gibbs free energy equation is given below:

$$g^{g}_{(T,p,y)} = \left[(1-y)\,g^{g}H_2O_{(T,p)} + y\,g^{g}NH_{3(T,p)} + RT\left[(1-y)\log_e(1-y) + y\log_e y\right]\right] \quad (8)$$

$$g^{g}_{H_2O(T,p)} = \left\{\begin{array}{l}h^{g}(T_o,p_o) - Ts^{g}(T_o,p_o) + \int C^{go}_{p}dT - T\int \frac{C^{go}_{p}}{Tdt} + RT\ln\frac{p}{p_o} + c_1(p-p_o) + c_2\left(\frac{p}{T^3} - 4\frac{p_o}{{T_o}^3} + 3\frac{p_oT}{{T_o}^4}\right) + \\ c_3\left(\frac{p}{T^{11}} - 12\frac{p_o}{{T_o}^{11}} + 11\frac{p_oT}{{T_o}^{12}}\right) + +c_3\left(\frac{p}{T^{11}} - 12\frac{p_o}{{T_o}^{11}} + 11\frac{p_oT}{{T_o}^{12}}\right) + \frac{c_4}{3}\left(\frac{p^3}{T^{11}} - 12\frac{{p_o}^3}{{T_o}^{11}} + 11\frac{{p_o}^3T}{{T_o}^{12}}\right)\end{array}\right\}_{H_2O} \quad (9)$$

Where

$$c^{go}_{p\,(T)} = d_1 + d_2T + d_3T^2$$

$$g^{g}_{H_2O(T,p)} = \left\{\begin{array}{l}h^{g}(T_o,p_o) - Ts^{g}(T_o,p_o) + d_1(T_o - T) + \frac{d_2}{2}\left({T_o}^2 - T^2\right) + \frac{d_3}{3}\left({T_o}^3 - T^3\right) + RT\log_e\frac{p}{p_o} + c_1(p - p_o) + c_2\left(\frac{p}{T^3} - 4\frac{p_o}{{T_o}^3} + 3\frac{p_oT}{{T_o}^4}\right) \\ + c_3\left(\frac{p}{T^{11}} - 12\frac{p_o}{{T_o}^{11}} + 11\frac{p_oT}{{T_o}^{12}}\right) + \frac{c_4}{3}\left(\frac{p^3}{T^{11}} - 12\frac{{p_o}^3}{{T_o}^{11}} + 11\frac{{p_o}^3T}{{T_o}^{12}}\right)\end{array}\right\}_{H_2O} \quad (10)$$

$$g^{g}_{NH_3(T,p)} = \left\{\begin{array}{l}h^{g}(T_o,p_o) - Ts^{g}(T_o,p_o) + d_1(T_o - T) + \frac{d_2}{2}\left({T_o}^2 - T^2\right) + \frac{d_3}{3}\left({T_o}^3 - T^3\right) + RT\log_e\frac{p}{p_o} + c_1(p - p_o) + c_2\left(\frac{p}{T^3} - 4\frac{p_o}{{T_o}^3} + 3\frac{p_oT}{{T_o}^4}\right) \\ + c_3\left(\frac{p}{T^{11}} - 12\frac{p_o}{{T_o}^{11}} + 11\frac{p_oT}{{T_o}^{12}}\right) + \frac{c_4}{3}\left(\frac{p^3}{T^{11}} - 12\frac{{p_o}^3}{{T_o}^{11}} + \frac{11{p_o}^3T}{{T_o}^{12}}\right)\end{array}\right\}_{NH_3} \quad (11)$$

Equation of state for pure components:

A. Specific Enthalpy at liquid and vapor phases

$$h^{l} = -RT_{B}T^{2}\left(\frac{\partial\left(\frac{g^{l}(T,p,x)}{T}\right)}{\partial T}\right)_{p,x} \tag{12}$$

$$h^{l} = -RT_{B}T^{2}\left\{(1-x)\frac{\partial}{\partial T}\left(\frac{g^{l}H_{2}O_{T,p}}{T}\right) + x\frac{\partial}{\partial T}\left(\frac{g^{l}NH_{3T,p}}{T}\right) + \frac{\partial}{\partial T}R\left[(1-x)\log_{e}(1-x) + x\log_{e}x\right] + \frac{\partial}{\partial T}\left(\frac{g_{E}(T,p,x)}{T}\right)\right\}_{p,x} \tag{13}$$

$$h^{l} = \left\{\begin{array}{l}\left(\frac{R}{18}\times T_{B}\right)\times(1-x)\times\left[h^{l}(To\ ,\ po) + b_{1}(T-T_{o}) + \frac{b_{2}}{2}\left(T^{2}-T_{o}^{2}\right) + \frac{b_{3}}{3}\left(T^{3}-T_{o}^{3}\right) + \left(a_{1}-a_{4}T^{2}\right)(p-p_{o}) + \frac{a_{2}}{2}\left(p^{2}-p_{o}^{2}\right)\right]_{H_{2}O} + \\ \left(\frac{R}{17}\times T_{B}\right)\times(x)\times\left[h^{l}(To\ ,\ po) + b_{1}(T-T_{o}) + \frac{b_{2}}{2}\left(T^{2}-T_{o}^{2}\right) + \frac{b_{3}}{3}\left(T^{3}-T_{o}^{3}\right) + \left(a_{1}-a_{4}T^{2}\right)(p-p_{o}) + \frac{a_{2}}{2}\left(p^{2}-p_{o}^{2}\right)\right]_{NH_{3}} + \\ \left[\frac{R}{(x\times 17 + (1-x)\times 18)}\times T_{B}\times(x)\times(1-x)\times\left(\left(e_{1}+e_{2}p+2\frac{e_{5}}{T}+3\frac{e_{6}}{T^{2}}\right)+(2x-1)\left(e_{7}+e_{8}p+2\frac{e_{11}}{T}+3\frac{e_{12}}{T^{2}}\right)+(2x-1)^{2}\left(e_{13}+e_{14}p+2\frac{e_{15}}{T}+3\frac{e_{16}}{T^{2}}\right)\right)\right]\end{array}\right\} \tag{14}$$

$$h^{g} = -RT_{B}T^{2}\left(\frac{\partial\left(\frac{g^{g}(T,p,y)}{T}\right)}{\partial T}\right)_{p,y} \tag{15}$$

$$h^{g} = -RT_{B}T^{2}\left\{(1-y)\frac{\partial}{\partial T}\left(\frac{g^{g}H_{2}O_{T,p}}{T}\right) + y\frac{\partial}{\partial T}\left(\frac{g^{g}NH_{3}T,p}{T}\right) + \frac{\partial}{\partial T}R\left[(1-x)\log_{e}(1-x) + x\log_{e}x\right]\right\}_{p,y} \tag{16}$$

$$h^{g} = \left\{\begin{array}{l}-\left(\frac{R}{18}\times T_{B}\right)\times(1-y)\times\left[\begin{array}{l}h^{g}_{(To,po)} + d_{1}(T-T_{o}) + \frac{d_{2}}{2}\left(T^{2}-T_{o}^{2}\right) + \frac{d_{3}}{3}\left(T^{3}-T_{o}^{3}\right) + c_{1}(p-p_{o}) + 4c_{2}\left(\frac{p}{T^{3}}-\frac{p_{o}}{T_{o}^{3}}\right) + \\ 12c_{3}\left(\frac{p}{T^{11}}-\frac{p_{o}}{T_{o}^{11}}\right) + 4c_{4}\left(\frac{p^{3}}{T^{11}}-\frac{p_{o}^{3}}{T_{o}^{11}}\right)\end{array}\right]_{H_{2}O} \\ -\left(\frac{R}{17}\times T_{B}\right)\times y\times\left[\begin{array}{l}h^{g}_{(To,po)} + d_{1}(T-T_{o}) + \frac{d_{2}}{2}\left(T^{2}-T_{o}^{2}\right) + \frac{d_{3}}{3}\left(T^{3}-T_{o}^{3}\right) + c_{1}(p-p_{o}) + 4c_{2}\left(\frac{p}{T^{3}}-\frac{p_{o}}{T_{o}^{3}}\right) + \\ 12c_{3}\left(\frac{p}{T^{11}}-\frac{p_{o}}{T_{o}^{11}}\right) + 4c_{4}\left(\frac{p^{3}}{T^{11}}-\frac{p_{o}^{3}}{T_{o}^{11}}\right)\end{array}\right]_{NH_{3}}\end{array}\right\} \tag{17}$$

B. Specific Entropy at liquid and vapor phases

$$s^{l} = -R\left(\frac{\partial g^{l}(T,p,x)}{\partial T}\right)_{(p,x)} \tag{18}$$

$$s^{l} = -R\left\{\frac{\partial}{\partial T}\left((1-x)g^{l}H_{2}O_{(T,p)} + xg^{l}NH_{3(T,p)} + RT\left[(1-x)\log_{e}(1-x) + x\log_{e}x\right] + g_{E(T,p,x)}\right)\right\}_{(p,x)} \tag{19}$$

On reduction the above equation (19) becomes

$$s^{l}=\left\{\begin{array}{l}\left[\frac{R}{18}\times(1-x)\left(s^{l}_{(To,po)}+b_1\log\left(\frac{T}{T_o}\right)+b_2(T-T_o)+\frac{b_3}{2}\left(T^2-{T_o}^2\right)+\left(-a_3-2a_4T\right)(p-p_o)\right)\right]_{H_2O}+\\ \left[\frac{R}{17}\times x\left(s^{l}_{(To,po)}+b_1\log\left(\frac{T}{T_o}\right)+b_2(T-T_o)+\frac{b_3}{2}\left(T^2-{T_o}^2\right)+\left(-a_3-2a_4T\right)(p-p_o)\right)\right]_{NH_3}-\\ \left[\frac{R}{x.17+(1-x).18}\times\frac{R}{x.17+(1-x).18}\times\left((1-x)\log_e(1-x)+x\log_e x\right)\right]+\left[\frac{R}{x.17+(1-x).18}\times x\times(1-x)\left(se_1+se_2+se_3\right)\right]\end{array}\right\} \quad (20)$$

Where

$$se_1=-e_3-e_4p+\frac{e_5}{T^2}+\frac{2e_6}{T^3}$$

$$se_2=(2x-1)\left(-e_9-e_{10}p+\frac{e_{11}}{T^2}+\frac{2e_{12}}{T^3}\right)$$

$$se_3=(2x-1)^2\left(\frac{e_{15}}{T^2}+\frac{2e_{16}}{T^3}\right)$$

$$s^{g}=-R\left(\frac{\partial g^{g}{}_{(T,p,y)}}{\partial T}\right)_{(p,y)} \quad (21)$$

$$s^{g}=-R\left\{\frac{\partial}{\partial T}\left((1-y)g^{g}{}_{H_2O(T,p)}+y\,g^{g}{}_{NH_3(T,p)}+RT\left[(1-y)\log_e(1-y)+y\log_e y\right]+g_{E(T,p,y)}\right)\right\}_{(p,y)} \quad (22)$$

$$s^{g}=\left\{\begin{array}{l}\left[-\frac{R}{18}\times(1-y)\left(-s^{g}_{(To,po)}-d_1\log\left(\frac{T}{T_o}\right)+\frac{d_2}{2}(2T_o-2T)+\frac{d_3}{2}\left({T_o}^2-T^2\right)+\frac{R}{18}\log\left(\frac{p}{po}\right)+c_2\left(\frac{3p_o}{{T_o}^4}-\frac{3p}{T^4}\right)+c_3\left(\frac{11p_o}{{T_o}^{12}}-\frac{11p}{T^{12}}\right)+\frac{c_4}{3}\left(\frac{11{p_o}^3}{{T_o}^{12}}-\frac{11p^3}{T^{12}}\right)\right)\right]_{H_2O}+\\ \left[-\frac{R}{17}\times(y)\left(-s^{g}_{(To,po)}-d_1\log_e\left(\frac{T}{T_o}\right)+\frac{d_2}{2}(2T_o-2T)+\frac{d_3}{2}\left({T_o}^2-T^2\right)+\frac{R}{18}\log_e\left(\frac{p}{po}\right)+c_2\left(\frac{3p_o}{{T_o}^4}-\frac{3p}{T^4}\right)+c_3\left(\frac{11p_o}{{T_o}^{12}}-\frac{11p}{T^{12}}\right)+\frac{c_4}{3}\left(\frac{11{p_o}^3}{{T_o}^{12}}-\frac{11p^3}{T^{12}}\right)\right)\right]_{NH_3}\\ \left[-\left(\frac{R}{y.17+(1-y).18}\times\frac{R}{y.17+(1-y).18}\right)\times\left((1-y)\log_e(1-y)+y\log_e y\right)\right]\end{array}\right\} \quad (23)$$

C. Specific Volume of liquid and vapor phases

$$v^{l}=\frac{RT_B}{p_B}\left(\frac{\partial}{\partial p}g^{l}{}_{(T,p,x)}\right)_{(T,x)} \quad (24)$$

$$v^{g}=\left[\frac{RT_B}{p_B}\left\{(1-y)\left(\frac{\partial}{\partial P}g^{g}{}_{H_2O\ T,p,y}\right)+(y)\left(\frac{\partial}{\partial P}g^{g}{}_{NH_3\ T,p,y}\right)+\frac{\partial}{\partial P}RT\left[(1-y)\log_e(1-y)+y\log_e y\right]\right\}_{T,y}\right] \quad (25)$$

In the same manner specific volumes were solved.

$$v^{l}=\left\{\begin{array}{l}\left(\frac{R}{18}\times\frac{T_B}{100p_B}\times(1-x)\times\left(a_1+a_2p+a_3T+a_4T^2\right)\right)_{H_2O}+\left(\frac{R}{17}\times\frac{T_B}{100p_B}\times(x)\times\left(a_1+a_2p+a_3T+a_4T^2\right)\right)_{NH_3}+\\ \frac{R}{x.17+(1-x).18}\times\frac{T_B}{100p_B}\times x(1-x)\times\left(e_2+e_4T+(2x-1)e_8+e_{10}T+(2x-1)^2e_{14}\right)\end{array}\right\} \quad (26)$$

$$v^g = \frac{RT_B}{p_B}\left(\frac{\partial}{\partial p} g^g{}_{(T,p,y)}\right)_{(T,y)} \tag{27}$$

$$v^l = \frac{RT_B}{p_B}\left\{(1-x)\left(\frac{\partial}{\partial p} g^l{}_{H_2O\,T,p,x}\right)+(x)\left(\frac{\partial}{\partial p} g^l{}_{NH_3\,T,p,x}\right)+\frac{\partial}{\partial p} RT[(1-x)\log_e(1-x)+x\log_e x]+\frac{\partial}{\partial p} g_{E\,T,p,x}\right\}_{T,x} \tag{28}$$

$$v^g = \left\{\left(\frac{R}{18}\times\frac{T_B}{100p_B}\times(1-y)\times\left(\frac{R}{18}\times\frac{T}{p}\right)+c_1+\frac{c_2}{T^3}+\frac{c_3}{T^{11}}+\frac{c_4p^2}{T^{11}}\right)_{H_2O}+\left(\frac{R}{17}\times\frac{T_B}{100p_B}\times y\times\left(\frac{R}{18}\times\frac{T}{p}\right)+c_1+\frac{c_2}{T^3}+\frac{c_3}{T^{11}}+\frac{c_4p^2}{T^{11}}\right)_{NH_3}\right\} \tag{29}$$

RESULTS AND DISCUSSIONS

To reduce the tedious iterations required by the existing correlations in developing the temperature concentration graphs and finding the ammonia mole fraction of vapor phase alternate solutions were proposed and utilized. The results obtained were validated by the previous results and found to have close match. Figure-4 shows the bubble point temperature and dew point temperature curves at a specified pressure and for different concentrations. The bubble point temperature and dew point temperature values are identical at initial and final concentrations ensuring a closed curve. The simulated works were carried out in MATLAB which shows a closer match with the literature. This work requires less calculation and can be utilized for the thermodynamic properties.

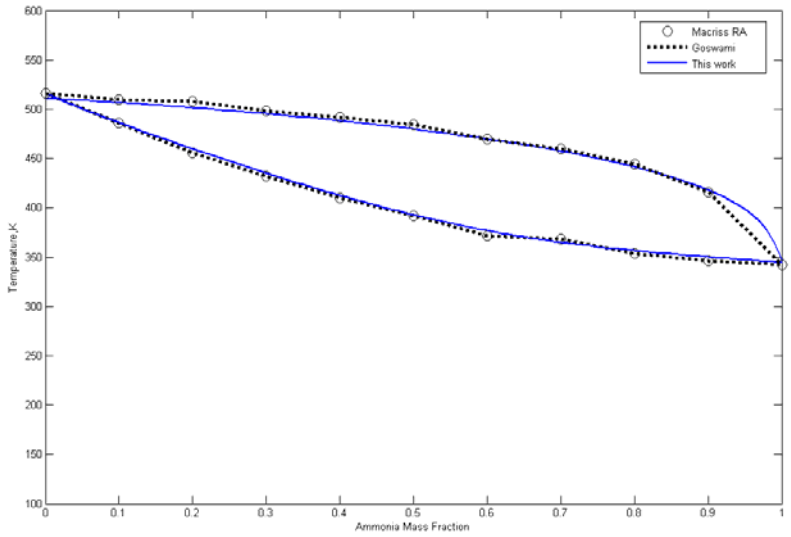

Figure-4. Bubble and dew point temperatures a 34.47 bar.

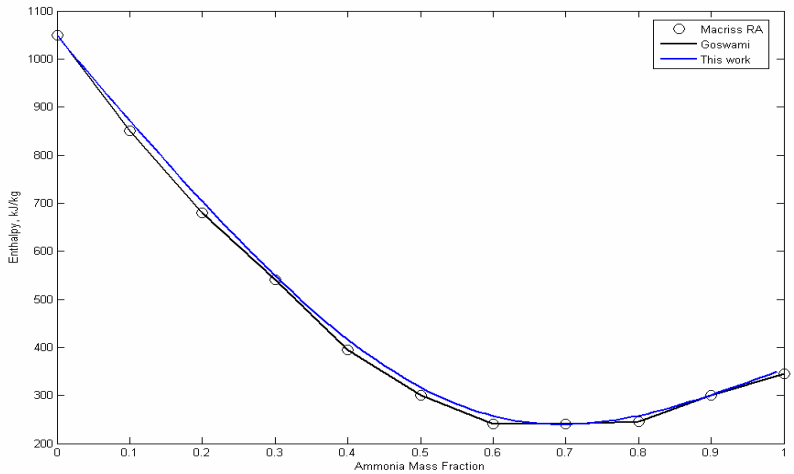

Figure-5. Enthalpy of saturated liquid at P=34.47 bar.

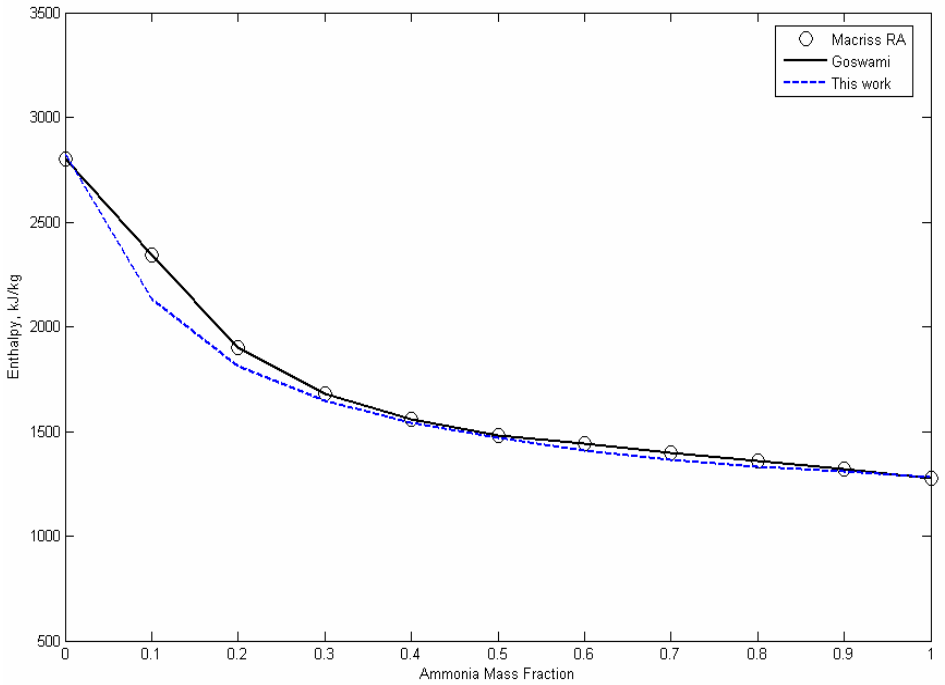

Figure-6. Enthalpy of saturated vapor at 34.47 bar.

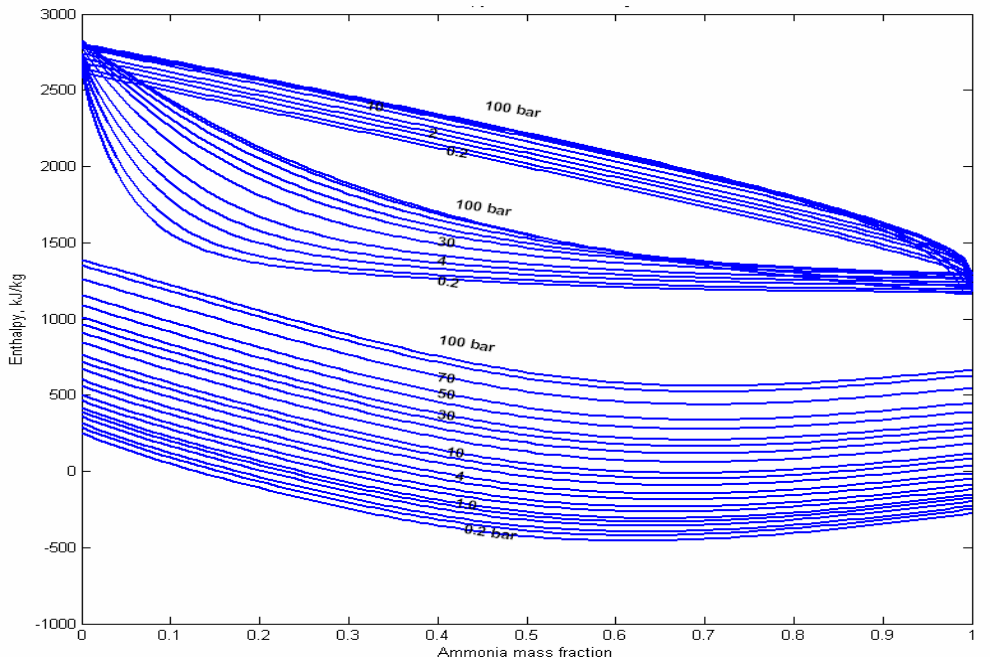

Figure-7. Ammonia-water enthalpy concentration diagram.

The liquid enthalpy and vapor enthalpy plots are shown in Figure-5 and Figure-6. From the Figure-5 the variation in the liquid enthalpy decreases first and then increases with increase in concentration and at a specified pressure. The results obtained were validated and shows a closer match with the compared results. Figure-6 shows the variation in the vapor enthalpy curve. The enthalpy value decreases continuously with the increase in the concentration. The enthalpy concentration with respect to the parameters pressure and concentration is shown in Figure-7.

Table-3. Conditions for temperatures at various values.

T °C	Condition	h_l kJ/kg	h_g kJ/kg	h kJ/kg	s_l kJ/kg-K	s_g kJ/kg-K	s kJ/kg-K	v_{lm} $^3/_{kg}$	$v_{g\,m}$ $^3/_{kg}$	V $_m$ $^3/_{kg}$
125	Compressed liquid	366.68	-	-	1.40	-	-	0.0015	-	-
138	Saturated liquid curve	435.95	-	-	1.57	-	-	0.0016	-	-
215	Two phase region-	-	-	1775.94	-	-	4.59	-	-	0.008
228	Saturated vapor curve-	-	1978.23	-	-	5.04	-	-	0.011	-
250	Superheated	-	2049.47	-	-	5.18	-	-	0.012	-

Table-3 specifies the condition for a particular temperature and gives the properties at that temperature.

The liquid enthalpy plot is obtained by considering the bubble point temperature and ammonia mole fraction of liquid phase. For plotting the auxiliary curve the liquid enthalpy is considered as a function of bubble point temperature and ammonia mole fraction of vapor phase. The ammonia mole fraction of vapor phase is obtained by correlation by Soleimani [17]. With the utilization of these correlations the result shows good agreement with the previous work.

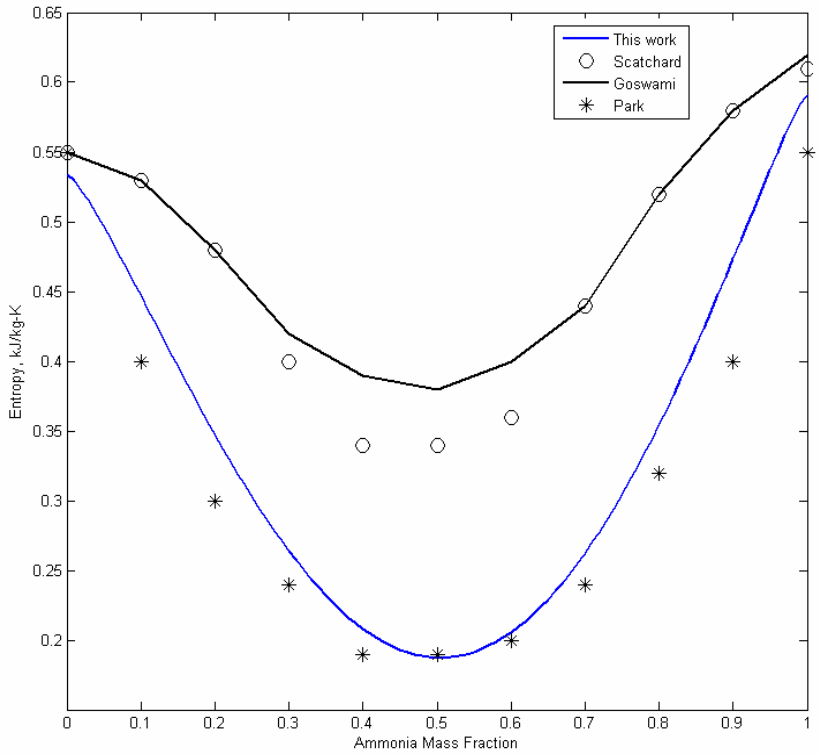

Figure-8. Entropy of saturated liquid at 37°C.

Figure-8. Shows the entropy of saturated liquid at a specified temperature and various concentrations. The entropy decreases and increases with the increase in concentration. The plot obtained is validated with the existing results and produces a good match. Whereas in the entropy of saturated vapor from Figure-9 at a specified temperature the plot decreases continuously with the increase in concentration.

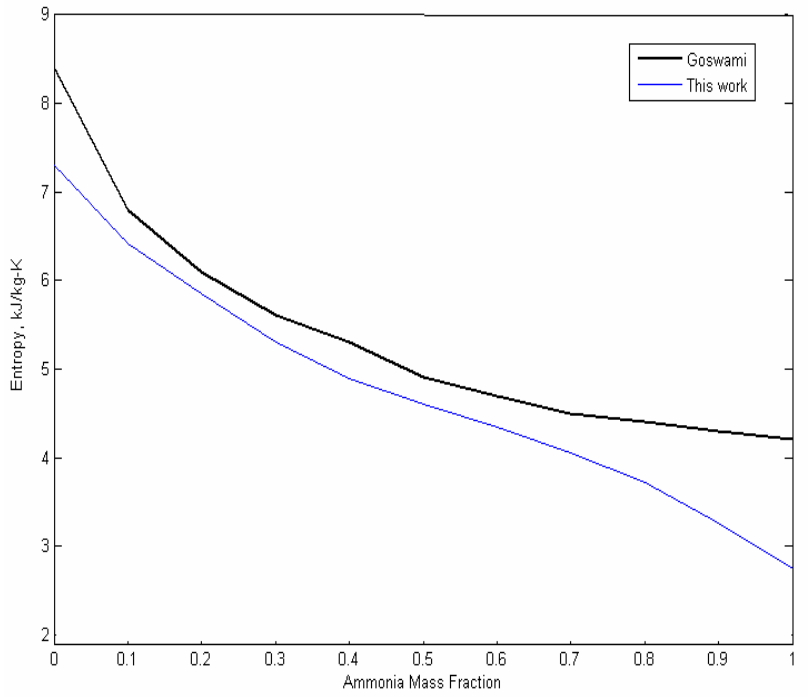

Figure-9. Entropy of saturated vapor at 37oC.

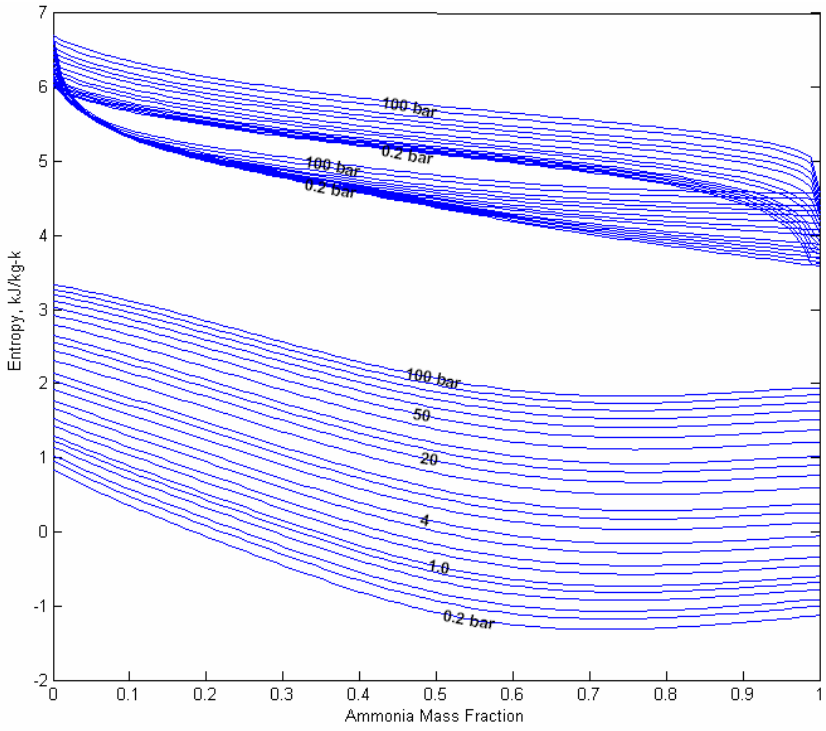

Figure-10. Entropy concentration diagram for ammonia-water mixture.

Figure-10 shows the entropy concentration diagram for ammonia - water mixture at various pressures and concentrations. The gap on the left hand side between the liquid curves are less compared with the gap on the right side of the plot which can be even extended to 150 bar with the same correlations. The values obtained by this plot can be utilized for any thermodynamic cycle. Upon increasing the pressures vapor curve and auxiliary curve are embedded one over the other forming a close gap between each other.

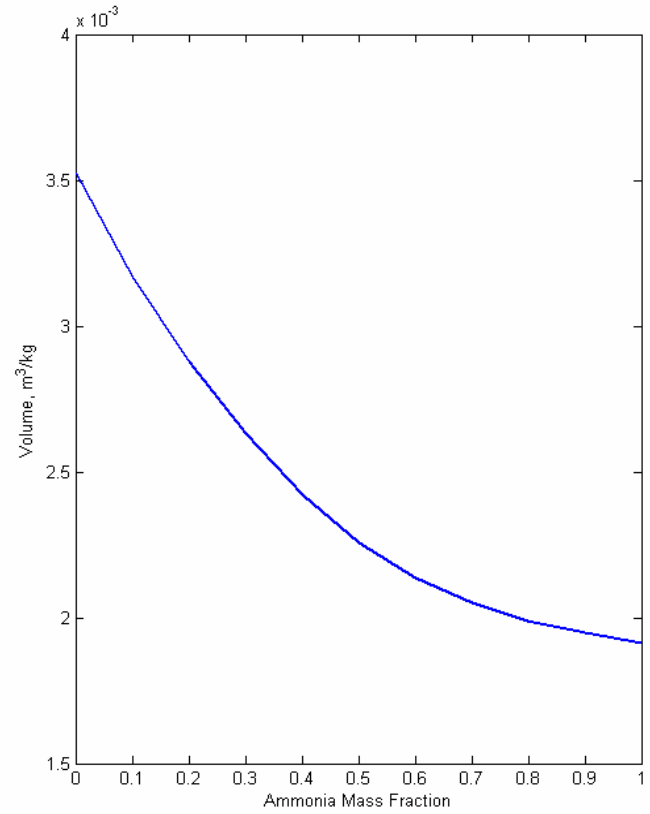

Figure-11. Volume of saturated liquid at P=34.47 bar.

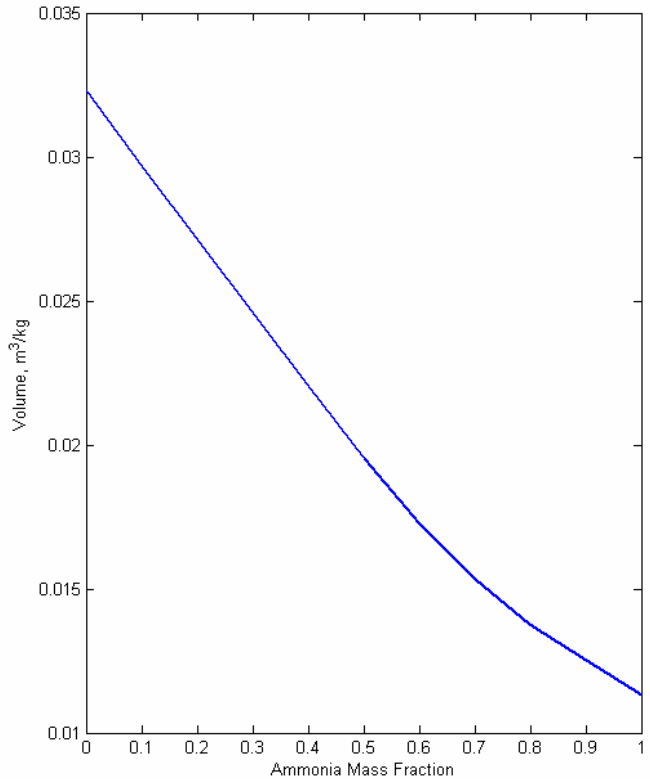

Figure-12. Volume of saturated vapor at P=34.47 bar.

Figure-11 and Figure-12 shows the liquid volume and vapor volume which has been derived utilizing bubble point temperature. With both the plots at a specified pressure the volume decreases with the increase in the concentration.

Exergy analysis is the maximum useful work obtained during an interaction of a system with equilibrium state. The total exergy of a system becomes a summation of physical exergy and chemical exergy [22].

$$E = E_{ch} + E_{ph} \quad (30)$$

$$E_{ph} = (h-h_o)-T_o(s-s_o) \quad [18] \quad (31)$$

$$E_{ch} = \left[\frac{x_i}{M_{NH_3}}\right] e^{o}_{ch,\,NH_3} + \left[\frac{(1-x_i)}{M_{H_2O}}\right] e^{o}_{ch,\,H_2O} \quad (32)$$

Where $e^{o}_{ch,\,NH3}$ and $e^{o}_{ch,\,H2O}$ are chemical exergies of ammonia and water. The standard chemical exergy of ammonia and water are taken from Ahrendts [21]

The exergy concentration plot for ammonia-water mixture at various pressures is shown in Figure-13. The liquid exergy curve decreases to certain concentration and approaches a near constant relation. The vapor exergy curve decreases continuously with the increase in concentration. The gap on the left hand side between the liquid curves are wider than the right hand side. The vapor exergy curve and auxiliary curves have identical values at initial and final concentrations which results in a closed loop. The space between the liquid exergy and the closed loop is reduced with the increase in pressures.

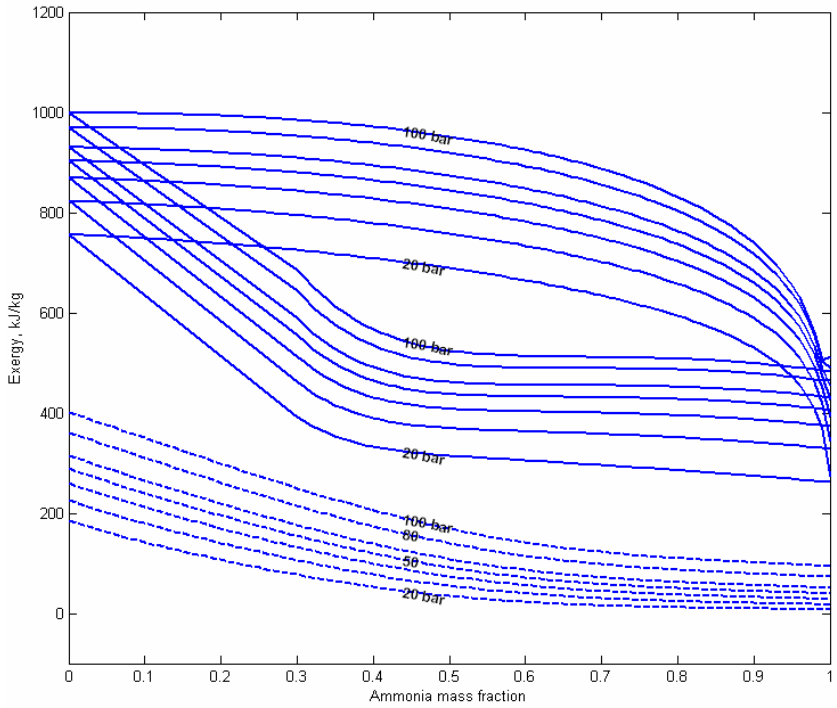

Figure-13. Exergy cncentration diagram for ammonia water mixture.

CONCLUSIONS

To develop thermodynamic properties of ammonia-water mixtures various correlations were analyzed. In this work three different correlations were utilized for developing the results. Bubble and dew point temperatures were obtained utilizing the correlation Patek and Klomfar [5], which reduces iterations which is been utilized for finding the properties enthalpy, entropy and volume. The properties were derived using relations Ziegler and Trepp [2]. The mole fractions of ammonia in vapor phase were solved with the correlation by Soleimani [17].

With the utility of these correlations the need of tedious iterations used in fugacity method were reduced. The results obtained in this work were validated by comparing with the published data and found closer matching. The exergy for the ammonia-water system have been simulated with the help of the derived properties to carryout the second law analysis to power systems.

REFERENCES

[1] Reid R. C., Prausnitz J. M. and Poling B. E. 1987. The Properties of Gases and Liquids. Fourth edition. New York, USA: McGraw-Hill. 667. ISBN 0-07-051799-1.

[2] B. Ziegler and Ch. Trepp. 1984. Equation of state for ammonia-water mixtures. Refrig. 7: 101-106.

[3] H. Renon J.L. Guillevic, D. Richon, J. Boston and H. Britt. 1985. A cubic equation of state representation of ammonia-water vapor-liquid equilibrium data. Refrig. 9: 70-73.

[4] J.P. Ruiter. 1990. Simplified thermodynamic description of mixtures and solutions. 13: 223-236.

[5] J. Patek and J. Klomfar. 1995. Simple functions for fast calculations of selected thermodynamic properties of the ammonia-water system. Refrig. 18: 228-234.

[6] Hasan Orbey, Stanley I. Sandler. 1995. On the combination of equation of state and excess free energy models. Fluid Phase Equilibria.111: 53-70.

[7] V. Abovsky. 1996. Thermodynamics of ammonia-water mixture. Fluid Phase Equilibria. 116: 170-176.

[8] Yousef S.H. Najjar. 1997. Determination of thermodynamic properties of some engineering fluids using two-consant equations of state. Thermochimica Acta. 303: 137-143.

[9] A. Nowarski and D.G. Friend. 1998. Application of the extended corresponding states method to the calculation of the ammonia-water mixture thermodynamic surface. International Journal of Thermophysics. 19: 1133-1141.

[10] Tillner-Roth. R, Friend. D.G. 1998. A Helmholz free energy formulation of the thermodynamic properties of the mixture, American Institute of Physics and American Chemical Society.

[11] Feng Xu, D. Yogi Goswami. 1999. Thermodynamic properties of ammonia-water mixtures for power-cycle applications. Energy. 24: 525-536.

[12] Raj Sharma, Diwakar Singhal, Ranjana Ghosh, Ashish Dwivedi. 1999. Potential applications of artificial neural networks to thermodynamics: vapor-liquid equilibrium predictions. Computers and Chemical Engineering. 23: 385-390.

[13] L.A. Weber. 1999. Estimating the virial coefficients of the ammonia-water mixture. Fluid Phase Equlibria. 162: 31-49.

[14] Eric W. Lemmon, Reiner Tillner-Roth. 1999. A Helmholtz energy equation of state for calculating the thermodynamic properties of fluid mixtures. Fluid Phase Equlibria. 165: 1-21.

[15] M. Barhoumi, A. Snoussi, N. Ben Ezzine, K. Mejbri, A. Bellagi. 2004. Modelling of the thermodynamic properties of the ammonia/water mixture. International Journal of Refrigeration. 27: 271-283.

[16] Kh. Mejbri, A. Bellagi. 2006. Modelling of the thermodynamic properties of the water-ammonia mixture by three different approaches. International Journal of Refrigeration. 29: 211-218.

[17] G. Soleimani Alamdari. 2007. Simple functions for predicing the thermodynamic properties of ammonia-water mixture. 20(1): 95-104.

[18] R. Senthil Murugan, P.M.V. Subbarao. Thermodynamic Analysis of Rankine-Kalina Combined Cycle. Int. J. of Thermodynamics. 11: 133-141.

[19] O.M. Ibrahim and S.A. Klein. 1993. Thermodynamic Properies of ammonia-water mixture. ASHRAE Trans. 99: 1495-1502.

[20] Vapor Absorption Refrigeration Systems Based on Ammonia-Water Pair. Version 1. ME, IIT.

[21] Ahredts. J. 1980. Reference states, Energy (5): 667-668.

[22] R.D. Mishra, P.K. Sahoo, A. Gupta. 2006. Thermoeconomic evaluation and optimization of an aqua-ammonia vapour-absorption refrigeration system. International Journal of Refrigeration. 29: 47-59.

Nomenclature

a_i, b_i, c_i, d_i, e_i	coefficients
m_i, n_i, ρ	coefficients
h	specific enthalpy, kJ/kg
s	specific entropy, kJ/kg-K
v	specific volume, m^3/kmol
T	temperature, K
p	pressure, bar
g	Gibbs free energy, kJ/kmol
c_p	specific heat capacity at constant pressure, kJ/kmol-K
R	universal gas constant, kJ/kmol-K
x	ammonia mole fraction in liquid phase
y	ammonia mole fraction in vapor phase

Superscripts		Subscripts	
g	gas phase	o	reference state
l	liquid phase	b	bubble point
o	ideal gas state	d	dew point